BIOSYSTEMS ENGINEERING 106 (2010) 260–267

Available at www.sciencedirect.com

ScienceDirect

journal homepage: www.elsevier.com/locate/issn/15375110

Research Paper

Development of an algorithm for online measurement of percent residue cover

F. Pforte*, O. Hensel

University of Kassel, Department of Agricultural Engineering, Nordbahnhofstr. 1a, D-37213 Witzenhausen, Germany

ARTICLE INFO

Article history:
Received 23 June 2009
Received in revised form
19 March 2010
Accepted 23 March 2010
Published online 15 May 2010

To develop the prototype of an online-capable camera sensor for measuring percent residue cover, appropriate image acquisition equipment and exposure conditions were investigated and different image processing algorithms for segmenting images into residue and soil were written with the help of commercial software. A large number of observations can easily be obtained using an online sensor, and this makes evaluation of its correct functioning by means of visual standard methods for estimating residue cover questionable. Hence an independent automatable approach was developed based on the analysis of features extracted from grayscale histograms of the residue images, which is even faster than the classical segmentation approach. The sensor was mounted onto an all-terrain vehicle (ATV) and the residue cover of three test fields was analysed. The Pearson correlation between the two measurement approaches was 0.967 for the cover rate observations taken on the three fields.

1. Introduction

Online determination of the percent residue cover by means of fast image processing is an unsolved problem. Although some investigations have reported the successful use of textural information (Han & Hayes, 1990) or single-pixel colour intensities (Morrison & Chichester, 1991) for segmenting images into background and residue, these methods depend on an operator who has to manually define specific features for each individual image. However an online system could offer substantial advantages for crop production: fast and simple documentation of the results of conservation tillage, use of the percentage mulch as an input parameter for different site-specific operations such as regulation of the working depth of a cultivator or variation of the sowing density of a seed drill (Hensel & Pforte, 2008). Different prototypes of an online camera sensor have been developed focussing on optimization of both image acquisition and processing. These prototypes were tested in field trials and compared with the results of visual standard methods for the determination of residue cover, yielding satisfactory correlation rates. An overview of the steps to achieve and assess the adequate performance of the camera sensor under practice conditions is given in this paper.

2. Material and methods

In contrast to the mapping-approach that is commonly used in precision farming (Hufnagel, Herbst, Jarfe, & Werner, 2004), the online approach implies a strong time-restriction on acquisition and processing of data. Considering usual working speed and implement sizes in conservation tillage, the processing time for straw-detection must not exceed

* Corresponding author. Tel.: +49 5542 981616; fax: +49 5542 981520.
E-mail address: florianpforte@uni-kassel.de (F. Pforte).
1537-5110/$ – see front matter © 2010 IAgrE. Published by Elsevier Ltd. All rights reserved.
doi:10.1016/j.biosystemseng.2010.03.014

approximately 1000 ms to ensure enough time for implement control. Because the number of image objects (straw particles) increases rapidly with percent residue cover, slow shape analysis operations must be limited as far as possible. Therefore the picture exposure conditions have to be optimized in order to yield as much desired information as possible from the unprocessed data.

2.1. *Image acquisition/equipment*

Different straw and soil samples were investigated by means of Reflectance Spectroscopy to identify the most suitable spectral range for distinguishing residue from the soil surface (Fig. 1a and b).

Spectra for Fig. 1a were taken in the laboratory from chopped wheat straw (collected some weeks after harvest), chopped barley straw (collected directly after harvest) and prepared earth (50% clay-silt soil, 50% 'Einheitserde' potting soil: a blend of 75% peat and 25% clay, Lab-colour: $L = 23.0$, $a = 3.5$, $b = 7.0$). For the reflectance measurements of the wet samples, the samples were saturated with water and briefly drained. The measurements were done in a dark room with the FieldSpec Pro JR field spectrometer (ASD Inc., Boulder, CO, USA) and a quartz tungsten halogen lamp (14.5V–50W) from JVC. For further instrumental details see Biewer, Erasmi, Fricke, and Wachendorf (2008). Spectra for Fig. 1b were taken with a RAMSES ARC radiometer (TriOS GmbH, Oldenburg, Germany). The spectra of top soil (clay-silt/shown as mean and standard deviation (STD)) were taken on 5 dates at separate locations near Hebenshausen, Germany between 2003 and 2004 (Döring, personal communication). Straw samples were cut straw from various sites in North Germany. For details of methods and soil type, see Döring, Kirchner, Kühne, and Saucke (2004). For the investigated samples, the spectra show a first maximum of the differences between straw and bare soil in the near infrared (NIR) between about 800 and 1400 nm. Therefore image acquisition was done with a visible light (VIS) blocking plastic polymer infrared filter (LP750, Eureca Messtechnik GmbH, Cologne, Germany) in front of the camera lens with a cut-on wavelength of 750 nm at which the transmission is 50% of the maximum.

For the first evaluation some cheap black & white complementary metal–oxide–semiconductor (C-MOS) and charge-coupled device (CCD) cameras, commonly used for surveillance-tasks, which are characterised by a high NIR-sensitivity below 1100 nm, were chosen as the sensor's eye. The percent residue cover was determined by algorithms written in the scientific image processing software Optimas from Media Cybernetics. In a first approach, the camera was mounted unsheltered at a height of about 1 m above the soil surface on an ATV serving as carrier vehicle; however, with this set-up the changing outdoor illumination conditions caused problems. Therefore a box was constructed around the camera to completely prevent the camera's field of view from being directly illuminated by sunlight in order to meet the required minimum image uniformity (Fig. 2). The base area of the box was 67 × 67 cm and the height 74 cm. The roof of the box (35 × 35 cm) was made of translucent, milky plastic foil and the surface of the interior walls consisted of the same foil glued on non-transparent, dark foil. The gap of about 30 cm between box and ground level was bridged by two rows of black plastic curtain attached to a 25 cm wide circumferential cantilever arm. Particularly under strong solar irradiation, the lighting conditions within the box were not fully homogeneous but sufficiently so for reliable image processing, as presented in the following sections. To ensure sufficient illumination also under cloudy conditions or in the dark, two 55 W twin-beam halogen tractor floodlights could be placed a variable distance (40–70 cm) above the roof of the box. These lamps were not used for the measurements described below. In order to achieve focused images at higher driving speeds ($\gtrsim 5$ km h^{-1}), it was necessary to control the exposure time of the camera. Thus a uEye-2220 USB2.0 CCD camera (1/2' monochrome sensor, 768 × 576 pixels, 50 frames s^{-1}) from Imaging Development Systems with a Pentax 4.8 mm F1.8 C-Mount lens was employed. All functions of the camera can be controlled directly from the chosen image analysis software via a software interface. A dialogue box was set up where the user could adjust the contrast, hardware gain and exposure time to be in a range uncritical for image sharpness before starting the automated image acquisition and processing. The imaged area of interest (AOI) could be chosen with a mouse

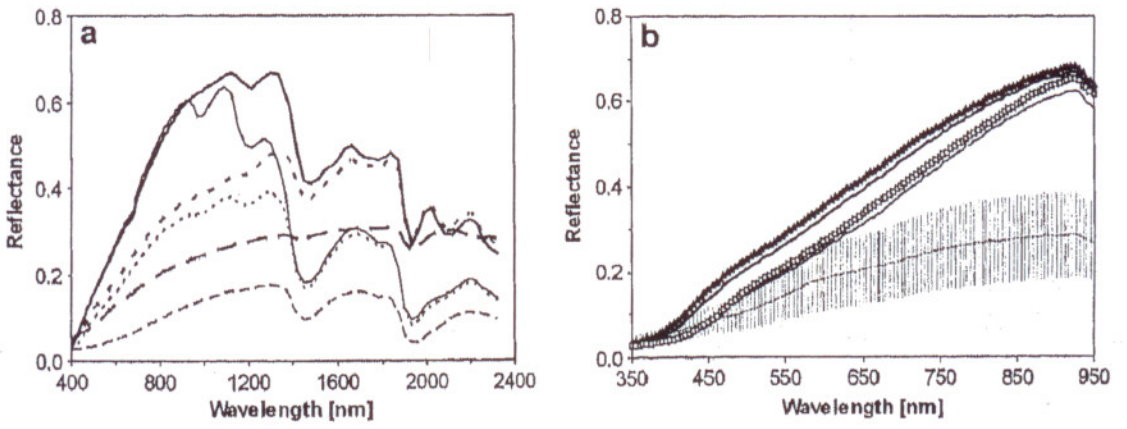

Fig. 1 – Reflectance spectroscopy shows a maximum difference between the investigated straw- and soil samples in the NIR; (a) — — bare soil dry, – – bare soil wet, —— barley dry, — barley wet, · · · wheat dry, · · · wheat wet, (b) ▲ rye, —— wheat1, — wheat2, □ barley, — soil (with STD); spectra in (b) by courtesy of T. Döring.

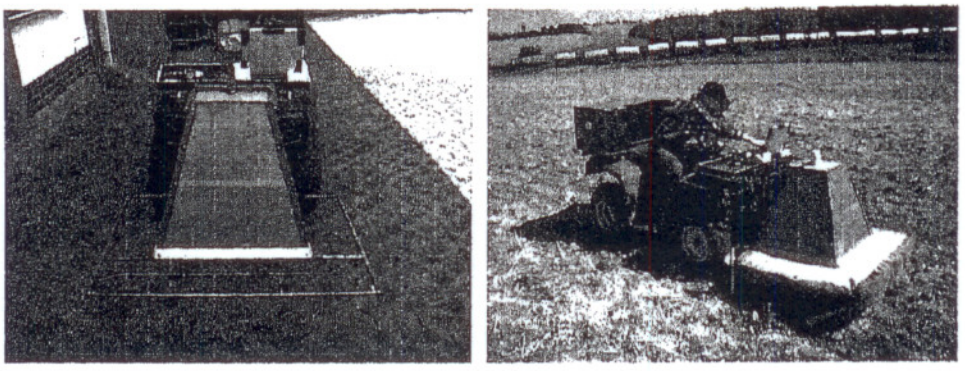

Fig. 2 – ATV with online camera sensor; the camera's field of view is protected from direct illumination by a box.

pointer. With the AOI about 55 × 55 cm (360 × 360 pixels) all parts of the box/curtains extending into the camera's field of view were excluded from the image, under all driving conditions.

2.2. *Image segmentation*

Under straightforward conditions, when the residues have a bright golden colour and are clearly silhouetted against dark soil, image processing can be reduced to the setting of a simple threshold to extract the percent residue cover with high accuracy, as confirmed by visual checking. In practice it is often more complicated due to exposure of the straw to weathering in the period since combining. The colours of soil and residue converge to some degree so that the threshold method is subject to significant error because a subset of soil particles ("background") is assigned to the mulch cover ("foreground") or vice versa. Hence an application of different convolution filters to the acquired images was tested to enhance the contrast between soil and residue. The combination of high-pass filters to accentuate the linear structure of typical straw particles and an average (low-pass) filter to eliminate to some degree the interfering microstructure of the soil turned out to be a powerful and fast tool for this purpose and has been used for the measurements presented in this paper. After this step the residue structure is made adequately accessible to highlighting by an automatic threshold in virtually all cases. The problem here is that no specific automatic threshold method works just as well for low and for high percent cover rates. This means that an automatable decision criterion is needed which roughly pre-estimates the coverage and selects an adequate threshold method for a more precise determination (Fig. 3). Thereafter some small soil structures which still may appear as foreground can be removed by a minimum boundary length condition and, if necessary, holes in the foreground structure can be closed. In a last step, the entire residue cover can easily be determined by calculating the area percentage of the remaining foreground phase.

For implementing the pre-estimation of the amount of coverage, a simple iterative approach has been chosen. After the convolution operations, an automatic threshold is set based on a method that yields a conservative estimate of the foreground phase, e.g. a method that minimises the classification error of two overlapping Gaussian bell curves which are fitted to the image grey-value histogram, one representing the light and one the dark objects respectively (Optimas manual, 1999). As already mentioned, the result might be quite imprecise, however together with the specification of a restrictive minimum boundary length condition (e.g. 5% of the entire image perimeter) for addressing only connected areas of a certain size, the sum of all remaining foreground areas can be taken as a first rough measure of the degree of coverage. Using this sum of foreground areas as input variable x of a branch function, the allocation to different thresholds can be realised by setting an appropriate boundary value x_{bound} which divides "high" and "low" covers. Since for high covers the minimisation within segment variance method, also known as the Method of Otsu (1979), shows clear advantages over other automatic thresholds, this method is applied for $x \geq x_{bound}$. For $x < x_{bound}$ again the minimisation of classification error method was chosen. It is crucial to place the change-over point in a transition range where both thresholding methods produce approximately the same segmentation result.

According to visual random sampling, this approach generates quite precise measurements for the whole range of residue covers under the exposure conditions provided by the protection box and has been used for the results shown in the

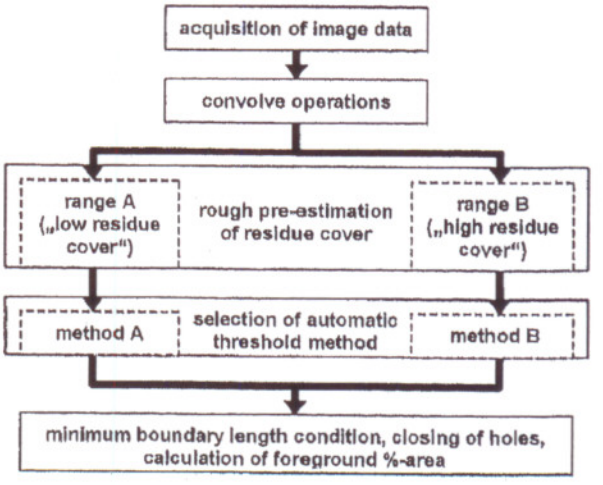

Fig. 3 – Schematical diagram of the algorithm for determination of percent residue cover.

following section. Under the conditions discussed above, the image acquisition and processing does not exceed the critical mark of 1000 ms, whereas the limitation of image resolution is of particular importance.

2.2.1. *Alternative processing approach as control*

Since the large number of observations easily obtained by online image analysis makes it difficult if not impossible to evaluate the correct functioning of the sensor for the wide range of practice conditions with the help of visual standard methods for estimating residue cover, it would be desirable to have an automatable control which is based upon an alternative approach. The basic idea for such a control is to use features of the grayscale 8 histograms (256 grey levels) of a set of images taken from covered soil to rank each individual image in terms of quantity of residue cover. The top row of Fig. 4 shows four sections of a field surface covered with amounts of straw increasing from (a) to (d). The percent cover was extracted from the associated processed binary images in the centre row. The bottom row shows the grayscale histograms of the unprocessed images. For low coverage, the majority of image pixels belongs to bare soil thus the envelope of the histogram resembles a bell-shaped curve with a maximum at the mean grey value of the soil (a). With increasing cover also the fraction of relatively bright pixels related to residue increases so that a second peak at a higher grey level appears in the histogram (b and c). At a certain point the bright pixels dominate the histogram so that the residue peak becomes higher than the soil peak (d).

Since the shape of a probability distribution is closely connected to its first four central moments, these are of special interest. These four moments, or variables derived therefrom, are mean, variance, skew and kurtosis respectively (Pollard, 1979). Notionally the mean can be expected to increase with increasing cover. The variance should have a maximum for medium cover rates around 50% where the histogram consists of two overlapping peaks, and minima for very low and high cover rates respectively. Instead of the variance, its square root, the standard deviation (STD), will be used in the following. Skewness is a measure of the asymmetry of a distribution: thus it is easy to visualize how the enveloping histogram curve changes from right-skewed (positive values of skew, most pixels dark) to left-skewed (negative values of skew, most pixels bright) as the cover changes from low to high. Kurtosis is a measure of the peakedness so it should change from relatively high values for the pointed ("leptokurtic") single-peak distributions at low and high covers to low or even negative values for the more oblate ("platykurtic") distributions at medium covers.

2.2.2. *Limits of methods*

Other published papers (e.g. Daughtry, 2001) have shown that residues can also be darker than soils in the VIS and NIR region depending on soil type, age of the residue and moisture conditions. The use of the technique presented here will therefore be limited to conditions where the contrast of residue and soil is not too low. Since edge-detection is used to further enhance the contrast between soil and residue, the technique might also be limited to spicular residues like cereal straw. As the time frame between combining and the following soil cultivation is relatively short (below approximately 4 weeks), it is expected

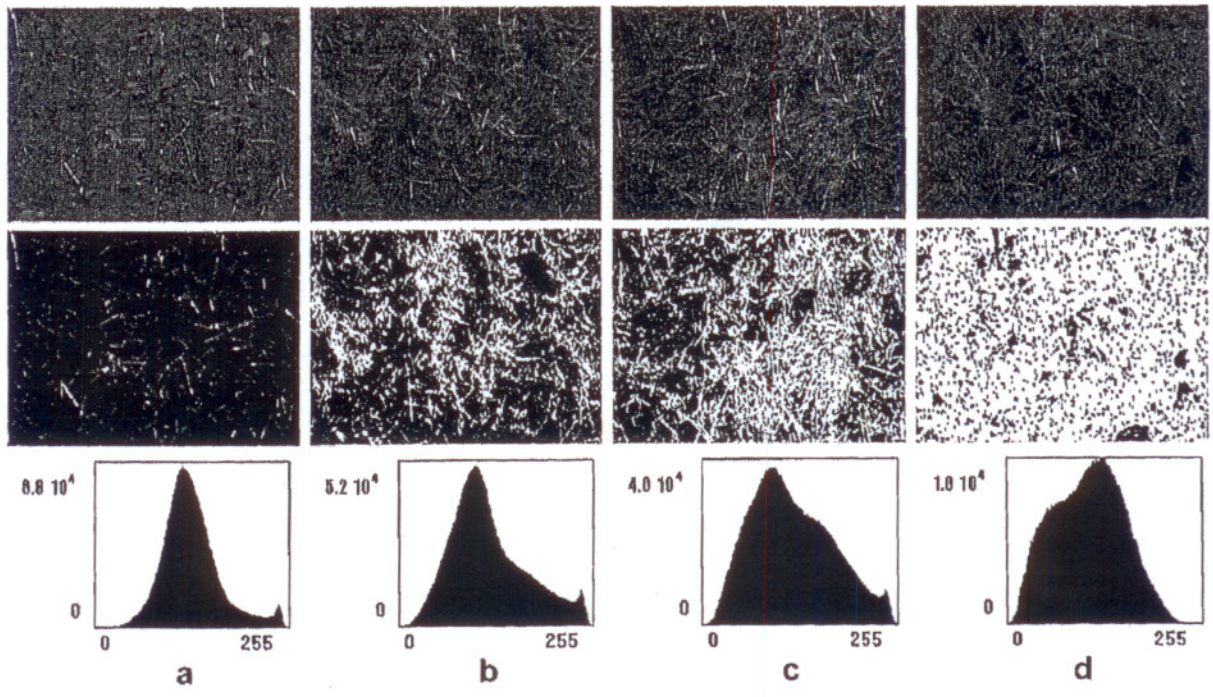

Fig. 4 – Top row: grayscale images of a field surface with residue cover increasing (a)–(d), centre row: segmentation of the images into residue and soil by means of image processing (%-cover: (a) 7.8%, (b) 39.1%, (c) 51.5%, (d) 78.4%), bottom row: grayscale histograms of the original images: with increasing coverage a "residue-peak" appears above the "soil-peak".

Table 1 – Analysis of the %-residue cover measured on three different fields.

Field	Mean cover [%]	Maximum [%]	Minimum [%]	Standard error	No. of samples	Test of normality[a]
Dynadrive: 3 cm residue: rye	57.76	87.21	31.33	0.775	224	$p = 0.043$
1st Tillage field cultivator: 5 cm residue: triticale	28.47	58.78	6.64	0.940	170	$p = 0.018$
2nd Tillage field cultivator: 10 cm residue: winter barley	16.69	53.74	3.31	0.715	132	$p = 0.001$

a Kolmogorov–Smirnov-Test, level of significance for normality usually at $p \geq 0.05$.

that the straw will usually remain comparatively bright and fresh so that optical contrast between soil and the major part of the residue will not have deteriorated to levels below detection thresholds.

3. Results and discussion

3.1. *Frequency distributions of percent cover*

The camera sensor was tested after harvest of the grain crop on three different fields of an organic farm that has been managed under a conservation regime for a long time. The farm has clay-silt soils and is situated in the same area (northern Hesse) as the sites on which the spectra for Fig. 1b were taken. The fields were chosen according to increasing tillage intensity: rye straw after shallow tillage with a Dynadrive (3 cm), triticale straw after primary tillage with a cultivator (5 cm), and winter barley straw after secondary tillage with a cultivator (10 cm). On each field, an area of 2–3 ha was investigated and the path of the ATV consisted of parallel lines a distance of about 15 m between each other. An image was acquired, saved and processed approximately every fifth second so that at an average driving speed of 9–10 km h^{-1} the distance between two sample points was about 13 m. Beside the obvious fact that the mean percent residue cover decreases with increasing tillage intensity, the cover was expected to be more or less normally distributed around this mean. This seems to be supported by Morrison, Lemunyon, and Bogusch (1995) who investigated a wide range of crop residues with the help of different visual methods and a large number of observations. To test this assumption, a statistical analysis of the entity of measured residue covers for each field was done. The results are shown in Table 1.

According to the test of Kolmogorov–Smirnov, for all sampling sites the totality of residue covers differed significantly from a normal distribution. However since normality tests are sensitive to features like skewness and kurtosis of an empiric distribution, an inspection of the histograms and Q–Q plots of the respective percent cover data, shown in Fig. 5, should be of more value in this case.

The normality plots as well as the histograms with superimposed bell curves suggest that the frequency distributions of the residue on the investigated fields are at least

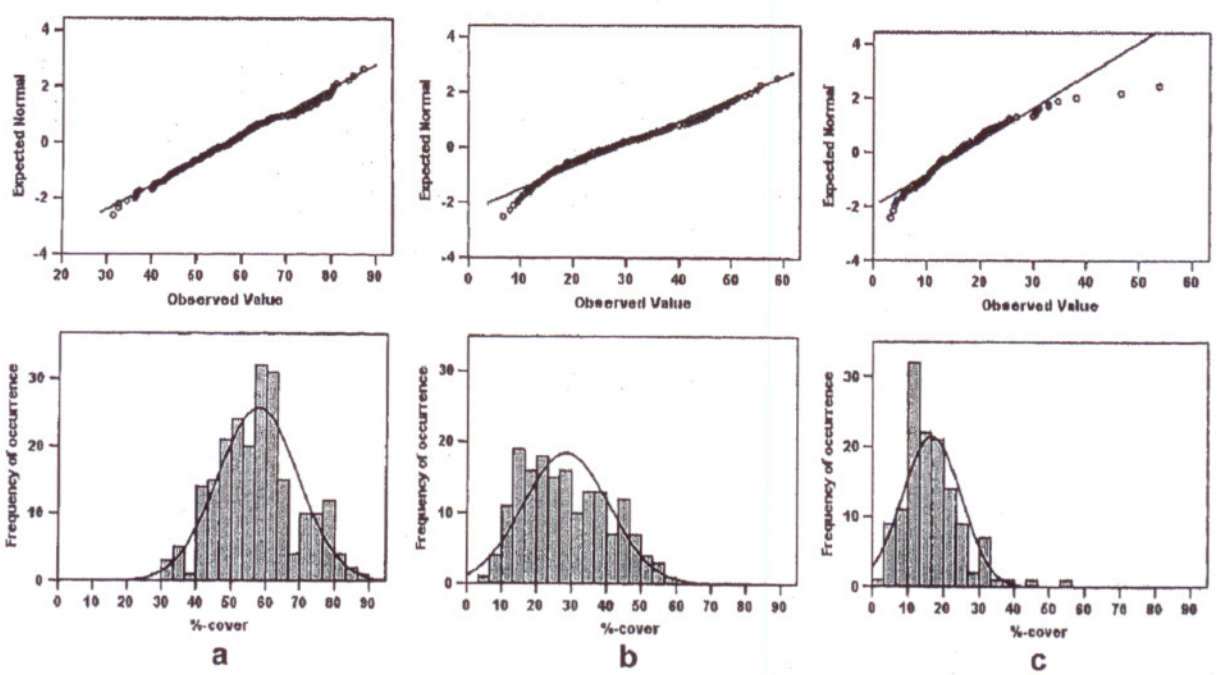

Fig. 5 – Normal Q–Q plots and histograms of measured percent residue covers for each of the three test fields, tillage intensity increasing left to right: (a) rye ~3 cm/mean cover: 57.76%, (b) triticale ~5 cm/28.47%, (c) barley ~10 cm/16.69%.

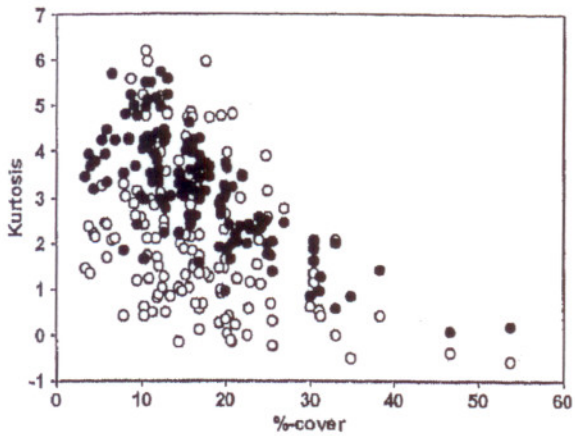

Fig. 6 – Kurtosis of the grayscale histograms of the images taken on barley residue plotted against the residue cover determined by online image processing: ○ images not standardized, ● images standardized; for the standardized images the kurtosis follows the expected trend more clearly.

comparatively close to normality. This can be seen as a first hint that the algorithm produces relatively reasonable results for the entity of sampling points, though it seems to suggest deficiencies in the algorithm might explain the partially distinct deviations from the ideal distribution. In particular, the apparently bimodal distribution of the rye residue with a valley below 70% cover seems to derive from a discontinuous change-over between the two automatic thresholding methods. To check this hypothesis, the pre-estimation process was disabled and all images taken on the rye field were analysed with help of the Otsu method. Since this yielded exactly the same histogram it can be concluded that the cover at all sampling points was too high to activate the "low cover" path with the alternative thresholding method so that the bimodality should not be caused by the image processing. On the other hand, there are other reasons for a deviation of the percent cover histogram from a normal distribution curve. Strictly speaking, normality can only be expected for the unlikely case of a homogeneous residue cover on the entire field before the respective tillage operation. Also the tillage operation itself influences the frequency of occurrence of a certain cover rate, e.g. it is known that the working speed directly affects the mixing of the residue (Estler & Knittel, 1996; Köller, 1981). Methods for measuring residue cover with help of the current visual standard are laborious, even with relatively small sample sizes as used in this paper. For this reason, little is known about typical distribution patterns of the histogram of cover rates related to certain tillage devices as shown in Fig. 5. Usually implement effects are characterised by the mean remaining residue cover estimated by comparatively few observations (e.g. Griffith & Wollenhaupt, 1994; Sloneker & Moldenhauer, 1977). Hůla, Šindelář, and Kovaříček (2005) have used image analysis of colour photographs to determine the residue cover left by different tillage equipment to find significant differences between the implements with the help of analysis of variance. Although the reported frequency distributions of percent cover for the single implements seem to be not unlike those shown above, they are based on only few measurements each.

3.2. *Analysis of histogram moments*

To check if the percent residue cover determined by online image processing correlates with the histogram features mentioned in Section 2, they were extracted systematically from the images taken on the three test fields and each plotted against the measured percent cover of the associated images. It turned out that in spite of the protection box, the illumination constraints were still too fluctuating to directly compare the values of histogram features of images taken over a period of several hours. In particular the measurements on the barley field were affected by permanently changing cloud cover. To diminish this source of error, the images were standardized by a localised luminance correction in the form of averaging over regions of 30 × 30 pixels before the computation of the histogram features. Fig. 6 illustrates the effect of this correction on the kurtosis data extracted from the images of barley residue.

After the standardization, the mean of the grayscale histograms showed the least reliable connection to the determined percent residue covers for the totality of

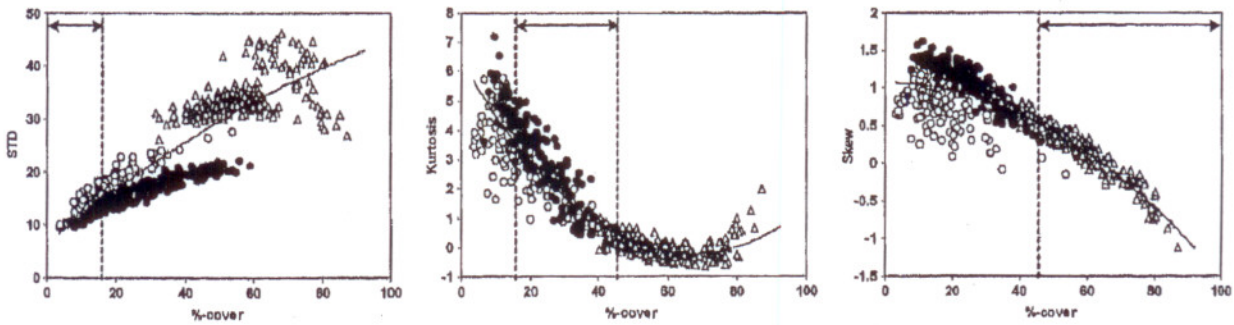

Fig. 7 – Left-right: standard deviation, kurtosis and skew extracted from the grayscale histograms of the standardized images taken on the three test fields, each plotted against the percent cover measured by online image analysis; second order polynomial curve fits are specified by parameters in Table 2; the vertical dotted lines and arrows indicate the co-domains corresponding with the most reliable domains of the inverse fit functions $(\mathrm{STD})^{-1}$, $(\mathrm{kurtosis})^{-1}$, $(\mathrm{skew})^{-1}$.

Table 2 – Specification of second order polynomial curve fits for the standard deviation, skew and kurtosis of the totality of standardized grayscale images taken on the three test fields.

Histogram feature	Coefficients			Adjusted R^2	Standard error
	a	b	c		
STD[a]	−0.002	0.543	6.572	0.792	4.401
Kurtosis[a]	0.001	−0.195	6.290	0.865	0.678
Skew[a]	0.3E-3	−4.8E-5	1.064	0.795	0.225

a No. of samples: 526.

measurements since it is directly sensitive to the absolute values of image luminance. Therefore a further consideration of the mean was abandoned. In contrast, the standard deviation, skew and kurtosis are only sensitive to the relative proportion of dark and bright pixels. This makes them more suitable for the desired application. In Fig. 7 these standardized histogram features are plotted against the percent cover measured on all of the three test fields by means of online image processing.

Apparently the standardized histogram features correlate well with the %-cover since they can be described by second order polynomial curve fits with reasonable error squares (Table 2). The curve fits are of the form $ax^2 + bx + c$ where x is the percent cover measured by image processing and a, b, c are real coefficients. Interestingly the standard deviation does not show the expected decrease for high cover values.

The presented curve fits, particularly those of skew and kurtosis, can be seen as an indication of the suitability of the presented image processing algorithm and sensor equipment to determine percent residue cover reasonably well for a wide range of practice exposure conditions. However a direct derivation of cover rates from only one of the polynomials using the respective underlying histogram data yields an unsatisfactory result. This is due to the fact that each of the fits possesses a characteristic extremal region where the necessary inverse function loses its definition. Hence, from the inverse of each polynomial, the most reliable domain of definition was chosen to derive the percent cover of the associated images: $(STD)^{-1}$ for low covers [0–16%], $(kurtosis)^{-1}$ for medium covers (16–46%), and $(skew)^{-1}$ for high covers [46–100%]. In Fig. 7 for each statistic, the borders of the corresponding range of cover values are indicated by vertical dotted lines. If the colours/luminances of soil and residue are shifting relative to one another, the locations of soil peak and residue peak in the image histogram will shift according to what affects the values of standard deviation, skewness and kurtosis. Hence for other soil–residue combinations with adequate contrast, the histogram feature distributions might look different. Therefore also the residue cover ranges which can be derived reliably from the different inverse curve fits should not be expected as generally constant.

Fig. 8a illustrates the correlation between the %-residue cover determined by "conventional" image processing and by using the inverse curve fits respectively. A close relation was found with a Pearson correlation of 0.967** (significant at the level ≤0.01). Also for comparison, the correlation between online image processing and a visual standard method is shown (Fig. 8b) which has been used to measure the percent cover at 65 GPS-referenced spots on 36 randomised parcels to which different amounts of straw cover and afterwards a shallow tillage had been applied (Wilhelm & Hensel, 2009). The visual method consisted of counting the intersections of a grid overlapping the residue and dividing the result by the total number of intersections (e.g. Hartwig & Laflen, 1978). For the grid a frame with 6 × 6 rope intersections and a mesh width of 10 cm was used and with its help the cover at each of the spots was estimated by three persons. Due to the lack of knowledge of the actual percent residue cover under field conditions, only statements can be made about how far a certain measuring procedure correlates with another one: in this case a Pearson correlation of 0.827** was found. However, in a laboratory test which provided well-defined percent cover rates, online image processing turned out to be the most suitable measurement method compared with different visual methods (Pforte & Hensel, 2008).

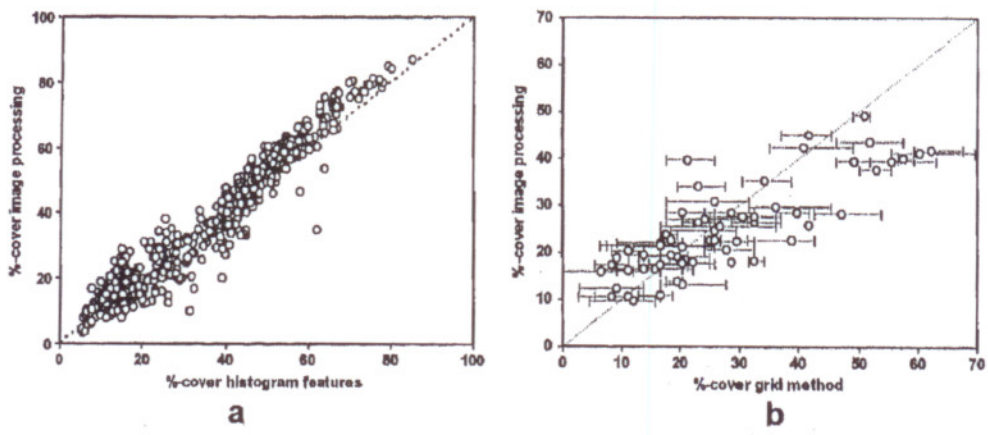

Fig. 8 – (a) Scatterplot of cover rates determined with the help of a combination of the curve fits shown in Fig. 7 versus "conventional" image processing, Pearson correlation: 0.967, (b) Cover rates measured by three persons counting grid intersections over residue in a field trial versus online image processing, Pearson correlation: 0.827**.**

4. Conclusions

Using a protection box around the camera for providing diffused light, the algorithm presented in this paper allows determination of percent residue cover in real time for a wide range of practical exposure conditions. However, the presented approach was validated only for conditions where the contrast of soil and the major part of residues was not too low. Since the frequency of occurrence of the measured percent cover is more or less normally distributed for the investigated fields, one can conclude on the one hand that the sensor produces reasonable results. On the other hand, such frequency distributions offer an easy and fast possibility for assessing the quality of work of different tillage equipment. However, a more detailed evaluation of the sensor's performance can be achieved by the investigation of the standard deviation, skew and kurtosis of the grayscale histograms of the standardized residue images that constitutes an alternative approach for measuring percent cover. Since a Pearson correlation of 0.967 between these methods was found, it seems possible to use the latter for the actual measurements and the "conventional" image processing only as control. This would result in a noticeable speed-up of the measurement because the extraction of histogram features consumes less processing time (≪1000 ms per image) than edge-enhancement and area related operations. For usability purposes, it would further be advantageous to get rid of the protection box. Among other things a future study is needed as to whether the histogram approach is also suitable under all exposure conditions or if a robust classical segmentation procedure would be favourable.

Acknowledgements

We thank Thomas Döring from The Organic Research Centre for providing straw and soil spectra.

Financial support from Deutsche Bundesstiftung Umwelt (DBU) is gratefully acknowledged.

REFERENCES

Biewer, S., Erasmi, S., Fricke, T., & Wachendorf, M. (2008). Prediction of yield and the contribution of legumes in legume-grass mixtures using field spectrometry. *Precision Agriculture*. doi:10.1007/s11119-008-9078-9. Online first.

Daughtry, C. S. T. (2001). Discriminating crop residues from soil by Shortwave Infrared Reflectance. *Agronomy Journal*, 93, 125–131.

Döring, T. F., Kirchner, S. M., Kühne, S., & Saucke, H. (2004). Response of alate aphids to green targets on coloured backgrounds. *Entomologia Experimentalis et Applicata*, 113, 53–61.

Estler, M., & Knittel, H. (1996). *Praktische Bodenbearbeitung*. Frankfurt: Verlagsunion Agrar. (in German).

Griffith, D. R., & Wollenhaupt, N. C. (1994). Crop residue management strategies for the midwest. In *Crops residue management*. Lewis Publishers.

Han, Y. J., & Hayes, J. C. (1990). Soil cover determination by image analysis of textural information. *Transactions of the ASAE*, 33(2), 681–686.

Hartwig, R. O., & Laflen, J. M. (1978). A meterstick method for measuring crop residue cover. *Journal of Soil and Water Conservation*, March–April, 90–91.

Hensel, O., & Pforte, F. (2008). *Sensor system for implement control in site-specific tillage*. Providence, Rhode Island (USA): ASABE AIM.

Hufnagel, J., Herbst, R., Jarfe, A., & Werner, A. (2004). *Precision farming*. KTBL-Schrift 419. Darmstadt: Kuratorium für Technik und Bauwesen in der Landwirtschaft e.V. (KTBL). (in German).

Hůla, J., Šindelář, R., & Kovaříček, P. (2005). Operational effects of implements on crop residues in soil tillage operations. *Research in Agricultural Engineering*, 51(4), 119–124.

Köller, K. (1981). *Bodenbearbeitung ohne Pflug*. Stuttgart: Verlag Eugen Ulmer. (in German).

Morrison, J. E., Jr., & Chichester, F. W. (1991). Still video image analysis of crop residue soil covers. *Transactions of the ASAE*, 34 (6), 2469–2474.

Morrison, J. E., Jr., Lemunyon, J., & Bogusch, H. C., Jr. (1995). Sources of variation and performance of nine devices when measuring percent residue cover. *Transactions of the ASAE*, 38 (2), 521–529.

OPTIMAS. (1999). *User Guide and Technical Reference*. Ver. 6.5. Silver Spring, MD: Media Cybernetics, L.P.

Otsu, N. (1979). A thresholding selection method from gray-level histograms. *Transactions on Systems, Man and Cybernetics*, 9, 62–66.

Pforte, F., & Hensel, O. (2008). Entwicklung einer automatisierbaren Referenzmethode zur Bestimmung des Bodenbedeckungsgrades bei der Mulchsaat. In *Proc. 66th Conference Agricultural Engineering (Land. Technik 2008)*. Düsseldorf: VDI Verlag. (in German).

Pollard, J. H. (1979). *A handbook of numerical and statistical techniques*. Archive Editions: Cambridge University Press.

Sloneker, L. L., & Moldenhauer, W. C. (1977). Measuring the amounts of crop residue remaining after tillage. *Journal of Soil and Water Conservation*, September–October, 231–236.

Wilhelm, B., & Hensel, O. (2009). Förderung der Mulchsaat im Ökolandbau – das Auflaufverhalten von Zwischenfrüchten. In *Proc. Beiträge zur 10. Wissenschaftstagung Ökologischer Landbau (Werte – Wege – Wirkungen: Biolandbau im Spannungsfeld zwischen Ernährungssicherung, Markt und Klimawandel)*. Berlin: Verlag Dr. Köster. (in German).